ЖЭТФ, 2025, том 167, вып. 3, стр. 371–378

THEORETICAL STUDY OF TERAHERTZ ABSORPTION SPECTRA AND NEUTRON INELASTIC SCATTERING IN FRUSTRATED MAGNET $Tb_2Ti_2O_7$

V. V. Klekovkina, **B. Z. Malkin***

Kazan Federal University
420008, Kazan, Russia

Received September 5, 2024
revised version October 15, 2024
Accepted for publication October 15, 2024

Using the single-particle approximation we calculate the envelopes of the spectral lines of terahertz absorption and inelastic neutron scattering spectra corresponding to magnetic dipole transitions between the sublevels of Tb^{3+} ions in the $Tb_2Ti_2O_7$ crystal, split by the field of random deformations induced by point defects of the crystal lattice upon violation of the stoichiometric composition of the crystal.

This paper is published as part of the Proceedings of the Spin Waves International Symposium («Spin Waves-2024»), Saratov, August, 2024.

DOI: 10.31857/S0044451025030083

1. INTRODUCTION

The spectral, thermodynamic and magnetic properties of geometrically frustrated terbium titanate compound $Tb_2Ti_2O_7$ with pyrochlore structure were actively studied for over 20 years. The system attracts much attention for the following reasons. Neighboring Tb^{3+} ions in $Tb_2Ti_2O_7$ are coupled by competing ferromagnetic exchange and antiferromagnetic dipole interactions (the Curie-Weiss temperature is $\Theta_{CW} = -13$ K [1]). According to theoretical studies the antiferromagnetic noncollinear phase of $Tb_2Ti_2O_7$ should be observed below temperatures of about 1.8 K [2]. However, magnetic ordering is not observed experimentally down to temperatures of 0.015 K [3]. The absence of magnetic ordering and the formation of a spin-liquid state (cooperative paramagnet) in $Tb_2Ti_2O_7$ is being discussed in the literature up to now.

The crystal lattice of terbium titanate with the pyrochlore structure belongs to the space symmetry group $Fd3m$ (face-centered cubic lattice). Tb^{3+} ions are in the Wyckoff position $16d$ $(1/2, 1/2, 1/2)$, Ti^{4+} ions are in the position $16c$ $(0, 0, 0)$, two sublattices O1 and O2 of O^{2-} ions are in the positions $8b$ $(3/8, 3/8, 3/8)$ and $48f$ $(x_0, 1/8, 1/8)$, respectively. Tb^{3+} ions form a network of corner-sharing tetrahedra. Four Tb^{3+} ions in a unit cell are crystallographically equivalent, but magnetically nonequivalent. The eight oxygen ions nearest to the terbium ion form a strongly distorted cube. The local point symmetry group of Tb^{3+} ion is trigonal D_{3d}.

In the crystal field of an ideal $Tb_2Ti_2O_7$, the ground multiplet $^7F_6$ of a Tb^{3+} ion is split into four doublets E_g and five singlets $3A_{1g} + 2A_{2g}$ (irreducible representations of the D_{3d} group are shown). The ground and the first excited states are non-Kramers doublets. The first excited energy level of the Tb^{3+} ion lies 13 cm^{-1} (0.39 THz) above the ground level [4, 5]. The remaining energy levels lie above 80 cm^{-1}. $Tb_2Ti_2O_7$ stands out among other isostructural rare-earth compounds by the small energy gap between the ground and the first excited sublevel of the ground multiplet. In other rare-earth pyrochlores, the first excited energy level is separated from the ground one by an energy gap of more than 70 cm^{-1}. Observations of extremely large values of magnetoelastic effects in $Tb_2Ti_2O_7$ at low temperatures, in particular, giant forced magnetostriction [6] and coupled electron-phonon excitations [7, 8], indicate an anomalously strong electron-lattice interaction. At present, it is generally accepted in the literature that it is the combination of these factors and

* E-mail: vera.klekovkina@gmail.com

the competition of ferromagnetic and antiferromagnetic interactions between neighboring Tb^{3+} ions that cause the absence of magnetic ordering in $Tb_2Ti_2O_7$ at low temperatures [9].

In the low-energy part of the inelastic neutron scattering spectra of $Tb_2Ti_2O_7$ single crystals and powders an intense line is observed in the energy range of about 1 cm^{-1} [10, 11]. In the terahertz absorption spectra a broad line is observed in the frequency range corresponding to energies of 10–18 cm^{-1} [12–14]. The specific profile of the inelastic neutron scattering spectrum in the range of low transfer energies (~ 1 cm^{-1}) and the fine structure of the terahertz absorption line indicate splitting of the ground and first excited non-Kramers doublets of the Tb^{3+} ion. This work is primarily aimed at clarifying the origin of these splittings.

The observed specific features of low-temperature spectral, magnetic and thermodynamic properties of $Tb_2Ti_2O_7$ powders and single crystals (absence of magnetic ordering, dependence of heat capacity and magnetic susceptibility on the sample [15, 16], violations of selection rules and additional lines in optical spectra [17], Raman and inelastic neutron scattering spectra) indicate the formation of microscopic inhomogeneities of the crystal lattice. Local static lattice deformations are induced during the synthesis of samples due to the formation of point defects: violations of the stoichiometric composition [18, 19] due to the mutual substitution of Ti^{4+} and Tb^{3+} ions, and oxygen vacancies characterized by the parameters x and y in the formula of the real compound $Tb_{2+x}Ti_{2-x}O_{7-y}$.

It should be noted that the interpretation of the specific shape of the terahertz absorption line at the transition between the lower non-Kramers doublets of Tb^{3+} ions proposed in [12–14], based on the consideration of coupled electron-phonon excitations, has no physical justification, since the hybridization of electron excitations within the states of the ground electron configuration with excitations of the cubic lattice (with phonons from the acoustic and odd optical branches of the vibrational spectrum) is possible (by parity) only at finite values of the phonon wave vectors, significantly exceeding the wave vectors of terahertz photons, which are close to zero.

2. CRYSTAL STRUCTURE DEFECTS AND THE FIELD OF RANDOM DEFORMATIONS

In the elastic continuum approximation, the structure of the crystal lattice at a distance r from a point defect (displacements of ions from equilibrium positions $\mathbf{u}(\mathbf{r}) \sim 1/r^2$ [20]) is described by a non-uniform deformation tensor with components $e_{\alpha\beta}(\mathbf{r}) \sim 1/r^3$. In the case of a finite concentration of defects, the components of the strain tensor are random variables with the probability distribution density of strains $g(\mathbf{e})$. In the general case, the structure of the multidimensional distribution function $g(\mathbf{e})$ is determined by the symmetry properties of the real crystal. When considering crystals of cubic symmetry, in particular, pyrochlores, the six-dimensional space of the components of the strain tensor can be decomposed into subspaces corresponding to irreducible representations A_{1g}, E_g and F_{2g} of the cubic symmetry group O_h:

$$e_1 = e(A_g) = (e_{xx} + e_{yy} + e_{zz})/\sqrt{6},$$
$$e_2 = e(E_g, 1) = (2e_{zz} - e_{xx} - e_{yy})/\sqrt{12},$$
$$e_3 = e(E_g, 2) = (e_{xx} - e_{yy})/2,$$
$$e_4 = e(F_{2g}, 1) = (2e_{xy} - e_{xz} - e_{yz})/\sqrt{6},$$
$$e_5 = e(F_{2g}, 2) = (e_{xz} - e_{yz})/\sqrt{2},$$
$$e_6 = e(F_{2g}, 3) = (e_{xy} + e_{xz} + e_{yz})/\sqrt{3}.$$

In an elastically isotropic continuum the trace of the strain tensor induced by point defects is zero [20], and the distribution function takes the form [21, 22]

$$g(\mathbf{e}) = \frac{2\gamma}{\pi^3} \sum_{m=2}^{6} \left(e_m^2 + \gamma^2\right)^{-3}. \tag{1}$$

The width of the distribution is determined by the parameter $\gamma = \frac{\pi(1+\sigma)}{27(1-\sigma)} C_{\rm d} |\Omega_0|$, where $C_{\rm d}$ is the number of defects per unit volume, Ω_0 is the "defect strength" and σ is the Poisson ratio. Calculations of the inelastic neutron scattering spectrum profile in the range of low transfer energies in $Tb_2Ti_2O_7$ [23] and $Pr_2Zr_2O_7$ [24] and of the low-temperature heat capacity of $Pr_2Zr_2O_7$ [24] using the distribution function (1) reproduced successfully the experimental data. The distribution function of deformations in an elastically anisotropic continuum, as was shown in [25], can be approximated by a generalized six-dimensional Lorentz function:

$$g(\mathbf{e}) = \frac{15\xi}{8\pi^3 \gamma_A \gamma_E^2 \gamma_F^3} \times$$
$$\times \left[\frac{e(A_{1g})^2}{\gamma_A^2} + \sum_{\lambda=1}^{2} \frac{e(E_g, \lambda)^2}{\gamma_E^2} + \sum_{\lambda=1}^{3} \frac{e(F_{2g}, \lambda)^2}{\gamma_F^2} + \xi^2 \right]^{-\frac{7}{2}}. \tag{2}$$

It should be noted that the distribution width for deformations of different symmetries depends on temperature, since the ratios between the measured elastic constants in $Tb_2Ti_2O_7$ change significantly in the

low-temperature range ($T < 80$ K) [26, 27]. The distribution function (2) was used in the calculations of the spectral and thermodynamic characteristics of the $Pr_2Zr_2O_7$ crystal in [28]. In the case of a high concentration of defects, the distribution function of deformations in an elastically isotropic continuum is transformed to the Gaussian form [21]. In particular, the Gaussian distribution function of random strains has been used in studies of the cooperative Jahn–Teller effects in solid solutions of rare-earth vanadates in [29]. In the present paper, the distribution function of deformations induced by point defects in the $Tb_2Ti_2O_7$ crystal is approximated by a generalized Gaussian distribution:

$$g(\mathbf{e}) = \frac{1}{\pi^3\xi^6\gamma_A\gamma_E^2\gamma_F^3} \times \exp\left\{-\left[\frac{e(A_{1g})^2}{(\gamma_A\xi)^2} + \right.\right.$$
$$\left.\left. + \sum_{\lambda=1}^{2}\frac{e(E_g,\lambda)^2}{(\gamma_E\xi)^2} + \sum_{\lambda=1}^{3}\frac{e(F_{2g},\lambda)^2}{(\gamma_F\xi)^2}\right]\right\}. \quad (3)$$

The widths ratio for distributions of deformations of different symmetries is suggested to be the same as in the case of the Lorentz distribution (parameters $\gamma_A = 1.2$, $\gamma_E = 31.8$, $\gamma_F = 24.8$ were calculated using the elastic constants of $Tb_2Ti_2O_7$ measured at a temperature of $T = 6$ K [30]). The parameter ξ depending on the type and concentration of defects was a fitting variable.

3. CRYSTAL FIELD AND ELECTRON-DEFORMATION INTERACTION

Calculations of energies of the Stark sublevels of Tb^{3+} ions in $Tb_2Ti_2O_7$ were performed using the numerical diagonalization of the Hamiltonian

$$H = H_{\rm FI} + H_{\rm CF},$$

defined in the full space of 3003 states of the electronic $4f^8$ configuration. Here $H_{\rm FI}$ is the standard Hamiltonian of a free ion [31], $H_{\rm CF}$ is the operator of interaction of $4f$-electrons with the static crystal field in the regular crystal lattice. The Hamiltonian $H_{\rm CF}$ of four magnetically nonequivalent Tb^{3+} ions in local Cartesian coordinate systems with Z axes along the local C_3 axes and X axes in the planes containing the Z axis and one of the crystallographic C_4 axes is determined by six non-zero real parameters B_p^k:

$$H_{\rm CF} = B_2^0O_2^0 + B_4^0O_4^0 + B_4^3O_4^3 + B_6^0O_6^0 + B_6^3O_6^3 + B_6^6O_6^6.$$

Here, O_p^k are linear combinations of spherical tensor operators, similar to Stevens operators [32] in the space of eigenfunctions of the angular momentum operator. Crystal-field parameters $B_2^0 = 213$, $B_4^0 = 368$, $B_4^3 = -2574$, $B_6^0 = 49.7$, $B_6^3 = 1218$, $B_6^6 = 100$ cm^{-1} were calculated within the framework of the exchange charge model [33] (the ion charges used in the calculation equal $q_{\rm Tb} = 2.82$, $q_{\rm Ti} = 3.58$, $q_{\rm O1} = -1.64$, $q_{\rm O2} = -1.86$, in units of elementary charge), parameters of charges on the bonds Tb-O1 and Tb-O2 equal $G_\sigma = G_s = G_\pi = 6.9$ and $G_\sigma = G_s = G_\pi = 10.5$, correspondingly.

Table 1. Calculated and measured energies of the Stark sublevels of the ground multiplet $^7F_6$ of Tb^{3+} ions in $Tb_2Ti_2O_7$ (cm^{-1}), corresponding irreducible representations of the D_{3d} group are indicated.

Γ	Theory	Experiment [4]	Experiment [5]
E_g	0	0	0
E_g	11.6	13	12.1
A_{2g}	82	83	82
A_{1g}	137	135	135
E_g	311	–	339
A_{2g}	385	–	–
A_{1g}	389	–	395
E_g	484	–	492
A_{1g}	566	–	–

The energies of the sublevels of the ground multiplet (see Table 1) and the g-factors of the ground ($g_\parallel = 10.5$) and the first excited ($g_\parallel = 13.6$) doublets obtained using the calculated crystal field parameters are in good agreement with the experimental data on IR absorption spectra [4], inelastic neutron scattering [5] and magnetization of $Tb_2Ti_2O_7$ in the external magnetic field [34].

When a point defect locally deforms the crystal lattice, the equilibrium positions of ions $\mathbf{R}(L,s)$ (L is the unit cell number and s is the ion number in the unit cell) shift by vectors $\mathbf{u}(\mathbf{R},s)$. As in the case of a uniformly deformed crystal, when considering a field of random deformations, we can introduce a deformation tensor with components $e_{\alpha\beta}$ and sublattice displacements $\mathbf{w}(s)$: $u_\alpha(L,s) = \sum_\beta e_{\alpha\beta}X_\beta(L,s) + w_\alpha(s)$. The crystal field parameters undergo increments $\Delta B_p^k = B_p^k(\mathbf{R}+\mathbf{u}) - B_p^k(\mathbf{R})$. Note, that we neglect here odd components of the crystal field induced by point defects which, in the case of local D_{3d} symmetry, can affect physical properties of rare-earth ions in the second order of the perturbation theory. However, odd local static lattice deformations, similarly to odd

Table 2. Parameters of the Hamiltonian of electron-deformation interaction (cm^{-1})

$p,\ k$	$\tilde{B}^k_p(A^2_{1g})$	$p,\ k$	$\tilde{B}^k_p(E^1_g,1)$	$\tilde{B}^k_p(E^2_g,1)$	$p,\ k$	$\tilde{B}^k_p(E^1_g,2)$	$\tilde{B}^k_p(E^2_g,2)$
2, 0	−8921	2, 1	10140	−8673	2, −1	10140	8673
4, 0	−1882	4, 1	2311	−5686	4, −1	2311	5686
4, 3	−14621	6, 1	2470	340	6, −1	2470	−340
6, 0	−483	4, 4	−2881	−7954	4, −4	−2881	7954
6, 3	4242	6, 4	−229	2077	6, −4	−229	−2077
6, 6	3546	2, 2	7501	−10960	2, −2	−7501	−10960
		4, 2	−2188	2760	4, −2	2188	2760
		6, 2	709	−982	6, −2	−709	−982
		6, 5	−615	3700	6, −5	615	3700

vibrational lattice modes, lift the ban on electric-dipole radiative transitions.

In the linear approximation in the components of the deformation tensor and the displacement vectors of the sublattices, the Hamiltonian describing the interaction of the Tb^{3+} ion with lattice deformations has the form [33]

$$H_{\text{el-def}} = \sum_{pk}\left[\sum_{\alpha\beta} B'^{k}_{p,\alpha\beta} e_{\alpha\beta} + \sum_{\alpha,s} B''^{k}_{p,\alpha}(s) w_\alpha(s)\right] O^k_p,$$

where

$$B'^{k}_{p,\alpha,\beta} = \frac{1}{2}\sum_{L,s}\left[X_\alpha(L,s)\frac{\partial}{\partial X_\beta(L,s)} + \right.$$

$$\left. + X_\beta(L,s)\frac{\partial}{\partial X_\alpha(L,s)}\right] B^k_p,$$

$$B''^{k}_{p,\alpha}(s) = \sum_L \frac{\partial B^k_p}{\partial X_\alpha(L,s)}.$$

The influence of sublattice displacements can be taken into account by renormalizing the parameters $\tilde{B}^k_{p,\alpha,\beta}$, and the Hamiltonian $H_{\text{el-def}}$ takes the form

$$H_{\text{el-def}} = \sum_{pk,\alpha\beta} \tilde{B}^k_{p,\alpha\beta} e_{\alpha\beta} O^k_p = \sum_{pk,\Gamma\lambda} \tilde{B}^k_p(\Gamma\lambda) e(\Gamma\lambda) O^k_p.$$

Renormalized parameters $\tilde{B}^k_p(\Gamma\lambda)$ of coupling with symmetrized components of the strain tensor $e(\Gamma\lambda)$, transforming along a row λ of the irreducible representation Γ, were obtained in our work [34] using the exchange charge model with subsequent corrections for better agreement with experimental data on the field dependence of forced magnetostriction and the temperature dependence of elastic constants. In the local coordinate system at the position of Tb^{3+} ions with the symmetry axis $C_3 \parallel [111]$, the Hamiltonian of the electron-deformation interaction takes the form $H_{\text{el-def}} = \sum_{\Gamma\lambda} V(\Gamma\lambda)\varepsilon(\Gamma\lambda)$, where $\varepsilon(\Gamma\lambda)$ are linear combinations of the deformation tensor components transforming in accordance with irreducible representations of the D_{3d} group,

$$\varepsilon(A^1_{1g}) = e(A_{1g}),\ \varepsilon(A^2_{1g}) = e(F_{2g},3),$$

$$\varepsilon(E^1_g,1) = e(E_g,1), \quad \varepsilon(E^1_g,2) = e(E_g,2),$$

$$\varepsilon(E^2_g,1) = e(F_{2g},1), \quad \varepsilon(E^2_g,2) = e(F_{2g},2),$$

and operators $V(\Gamma\lambda) = \sum_{pk} \tilde{B}^k_p(\Gamma\lambda) O^k_p$. The parameters of the electron-deformation interaction used in the present work are given in Table 2.

4. ABSORPTION SPECTRUM PROFILE

The absorption spectra of linearly polarized synchrotron radiation in the frequency range of 0.2–1 THz at temperatures of 6–300 K were measured on single-crystal samples of $Tb_{2+x}Ti_{2-x}O_{7-y}$ grown by the zone melting method [14]. The radiation field was directed along one of the trigonal ([111]) or rhombic ([1-10]) symmetry axes of the crystal with an alternating magnetic field $\mathbf{h} \parallel [11-2]$, $\mathbf{h} \parallel [1-10]$ or $\mathbf{h} \parallel [111]$, respectively, in crystallographic system of coordinates.

Comparing the low-temperature heat capacity measurements in the samples used in spectroscopic studies [12] to earlier results on temperature dependences of the heat capacity in a terbium titanate with different relative contents of Tb^{3+} and Ti^{4+} ions [35], one could estimate the value of the parameter x, which characterizes the deviation from the stoichiometric composition [12–14]. For samples with substantially different absorption spectra caused by electromagnetic

radiation-induced transitions of Tb^{3+} from the ground state (doublet E_g^1) to the nearest excited state (doublet E_g^2), the transition frequency in the crystal field was approximately 0.43 THz. In particular, in samples whose absorption spectrum at low temperatures contains a broad line of complex shape, corresponding to the transition $E_g^1 \Rightarrow E_g^2$, and an additional weak line of unknown nature at a frequency of 0.67 THz, the parameter x is approximately equal to -0.0025. Samples with $x > 0$ and $x < 0$ contain defects of various types. In crystals with $x > 0$, heterovalent substitution of Ti^{4+} ions by Tb^{3+} ions is accompanied by the appearance of vacancies in the oxygen sublattices; at $x < 0$, filling of the $8a$ positions by oxygen ions is possible.

Calculations of the absorption spectra of four magnetically nonequivalent Tb^{3+} ions at the vertices of the tetrahedron were performed based on the single-ion Hamiltonian in the corresponding local coordinate systems

$$H_{\rm t} = H + H_{\text{el-def}} + H_{\rm r},$$

where $H_{\text{el-def}}$ is the above-introduced operator of interaction of $4f$-electrons with the field of random deformations, and $H_{\rm r}$ is the operator of interaction with the radiation. Since zero-phonon optical electric dipole transitions between states of the electronic $4f^8$ shell in the crystal field of D_{3d} symmetry are forbidden by parity, only interactions with the radiation magnetic field are taken into account in the operator $H_{\rm r} = -\mathbf{M}\cdot\mathbf{h}$ ($\mathbf{M} = -\mu_{\rm B}(k\mathbf{L} + 2\mathbf{S})$ is the magnetic moment operator of a Tb^{3+} ion, $\mathbf{L}$ and $\mathbf{S}$ are the total orbital momentum and spin, respectively, $\mu_{\rm B}$ is the Bohr magneton, $k = 0.95$ is the orbital reduction factor).

In the general case, lattice deformations of E_g symmetry split each of the E_g^1 and E_g^2 doublets into two sublevels with energies $E_1(\mathbf{e})$ and $E_2(\mathbf{e})$, $E_3(\mathbf{e})$ and $E_4(\mathbf{e})$, respectively, and wave functions $|i(\mathbf{e})\rangle$ (i = 1-4); fully symmetric deformations shift the upper doublet relative to the lower one. Thus, at low temperatures in the space of four states of the two lower doublets there are six absorption channels with six spectral lines: P0 ($E1 \Rightarrow E2$), P1 ($E2 \Rightarrow E3$), P2 ($E2 \Rightarrow E4$), P3 ($E1 \Rightarrow E3$), P4 ($E1 \Rightarrow E4$), P5 ($E3 \Rightarrow E4$).

Considering the operator $H_{\rm r}$ as a time-dependent perturbation, we obtain the distribution of the absorption intensity of the radiation of frequency ω, caused by transitions between sublevels of terbium ions numbered with index s, with energies $E_{i,s}(\mathbf{e})$ and $E_{k,s}(\mathbf{e})$ for the fixed components of the deformation tensor $\mathbf{e}$, in the form

$$I(\omega,\mathbf{e}) = C\omega\sum_{s=1}^{4}\sum_{i=1}^{2}\sum_{k=3}^{4}[p_i(\mathbf{e}) - p_k(\mathbf{e})]\times \times |\langle i|\mathbf{M}_s\cdot\mathbf{h}_{0,s}|k\rangle|^2 I_{0,ik}(\omega,\mathbf{e}), \quad (4)$$

where C is the numerical factor, p_i is the population of the i-th state, $\mathbf{M}_s$ is the magnetic moment operator and $\mathbf{h}_{0,s}$ is the unit vector directed along the polarized radiation magnetic field in the local system of coordinates for the ion s, respectively,

$$I_{0,ik}(\omega,\mathbf{e}) = \frac{1}{\sqrt{2\pi}\sigma}\times \times \exp\left\{-\frac{[\omega - (E_k(\mathbf{e}) - E_i(\mathbf{e}))/\hbar]^2}{2\sigma^2}\right\} \quad (5)$$

is the Gaussian form-function of the spectral line corresponding to a separate transition with the dispersion $\sigma = 7.5\cdot 10^{-3}$ THz.

The absorption spectrum profile is obtained by averaging the distribution (4) with the deformation distribution function (3):

$$I(\omega) = \int I(\omega,\mathbf{e})g(\mathbf{e})\times \times de(A_{1g})\prod_{\lambda=1,2} de(E_g,\lambda)\prod_{\lambda=1,2,3} de(F_{2g},\lambda). \quad (6)$$

Numerical calculations of integrals (6) in a hyperspherical coordinate system in a six-dimensional space of strain tensor components with a frequency step $\Delta\omega = 3.75\cdot 10^{-3}$ THz ($T = 6$ K, $\mathbf{h} \parallel [11-2]$) are compared with the measured absorption spectrum (Fig. 3S in [14]) in Fig. 1. The calculation of the absorption spectrum profile is performed under the assumption that the intensity of the terahertz radiation source does not depend on the frequency. The value of the variable parameter $\xi = 6.5\cdot 10^{-4}$, as well as the presented above standard deviation σ in the form-function of optical transitions (5), were determined by comparing the calculated spectrum with the one measured in [14]. Figure 1 also shows the lines P1, P2, P3 and P4, the superposition of which determines the shape of the envelope of magnetic dipole transitions between the sublevels of the ground and first excited doublets of Tb^{3+} ions in a crystal field, split by random deformations. The optical transitions that form the lines P2 and P3, P1 and P4 are induced predominantly by projections of the field $\mathbf{h}$ onto the local planes XY and the Z axis, respectively. The ratio of the calculated sums of the intensities of the specified lines I(P2+P3)/I(P1+P4) = 1.4 agrees

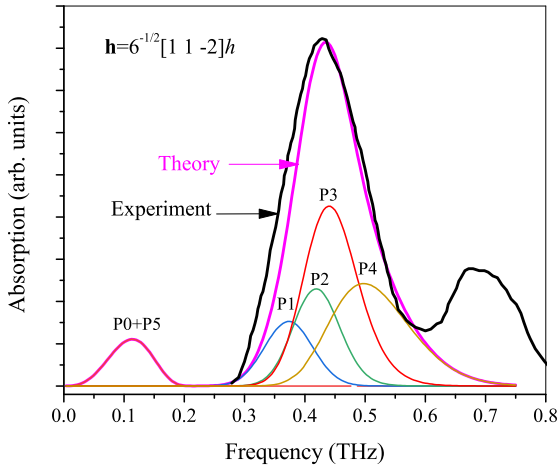

Fig. 1. Calculated absorption spectrum profile of linearly polarized radiation of the $Tb_2Ti_2O_7$ single-crystal in comparison with experimental data [14] at a temperature $T = 6$ K

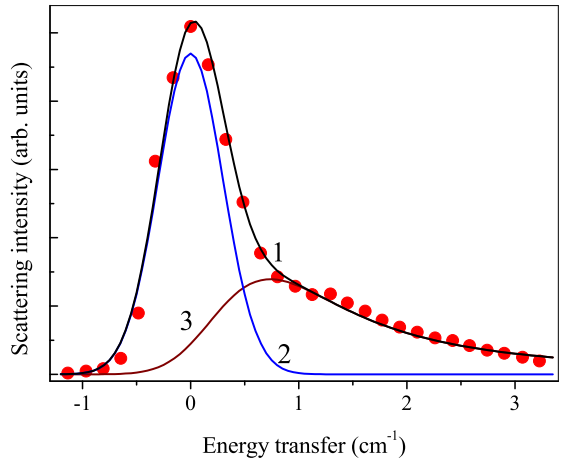

Fig. 2. Measured (symbols) [10] and calculated (line 1) neutron scattering spectra of the $Tb_2Ti_2O_7$ crystal at $T = 0.07$ K. Lines 2 and 3 correspond to the contributions of elastic and inelastic scattering

qualitatively with the ratio of the squares of the modules of the matrix elements of the projections of the magnetic moment on the X and Z axes on the wave functions of the doublets E_g^1 and E_g^2 in the crystal field of the regular lattice $|M_X(1,3)/M_Z(1,4)|^2 = 1.7$ (the matrix elements of the operators M_X and M_Y are equal in module), however, the calculations performed do not reproduce the dependence of the absorption spectrum profile on the orientation of the field $\mathbf{h}$ in the crystallographic coordinate system observed in the measured spectra.

An additional line in the frequency range 0.7 ± 0.05 THz, observed in the measured spectrum, corresponds to the absorption of radiation by Tb^{3+} ions located either in Ti^{4+} positions or closest to a point defect that strongly changes the crystal field in neighboring lattice sites.

The P0+P5 line in Fig. 1 with the P0 line contribution dominating at low temperatures, represents the envelope of transitions between the sublevels of E_g^1 and E_g^2 doublets split by random deformations. It should be noted that the splitting of the doublet is reproduced by calculation only when using a multi-dimensional (at least two-dimensional when considering deformations of E_g symmetry [21]) distribution function with the most probable non-zero value of the vector modulus with components equal to the degenerate deformations, $|\mathbf{e}(\Gamma)| = \left[\sum_\lambda e(\Gamma,\lambda)^2\right]^{1/2}$, $\Gamma = E_g, F_{2g}$.

The splitting of the ground doublet $\Delta(\mathbf{e})$ of Tb^{3+} ions in $Tb_2Ti_2O_7$ crystals of an order of 1–2 cm^{-1} was recorded in high-resolution inelastic neutron scattering spectra [10, 36] at low temperatures. The presence of a broad tail of the intense line in the region of quasi-elastic neutron scattering with transfer energies close to zero (see Fig. 2) indicates a Lorentzian distribution of random deformations in the studied samples, apparently with a small deviation from the stoichiometric composition. In this paper we calculated the intensity distribution in the inelastic neutron scattering spectrum averaged over scattering vectors

$$I_{\text{inelast}} \sim \int \exp\left[-\frac{(E-\Delta(\mathbf{e}))^2}{2\delta^2}\right] g(\mathbf{e})d\mathbf{e},$$

using the strain distribution function (1) in the form of a generalized Lorentz function with the width $\gamma = 5.5 \cdot 10^{-4}$, the dependence of the splitting of the doublet $\Delta(\mathbf{e})$ on the components of the strain tensor was obtained using the considered above Hamiltonian of the electron-deformation interaction. The observed neutron scattering spectrum profile is well reproduced by the sum of the intensities of the inelastic scattering and elastic scattering spectra, in which the intensity distribution was approximated by a Gaussian form-function $I_{\text{elast}} \sim \exp\left(-E^2/2\delta^2\right)$ with the standard deviation $\delta = 0.3$ cm^{-1} (see Fig. 2).

It should be noted that practically similar results of the calculation of the inelastic neutron scattering spectrum were obtained by taking into account the elastic anisotropy of the terbium titanate lattice using the random deformation distribution function (2) with a width of $\xi = 2.6 \cdot 10^{-5}$.

5. CONCLUSIONS

In this work, we calculated the envelopes of low-temperature absorption spectra of linearly polarized terahertz radiation and inelastic neutron scattering in the absence of external magnetic fields in $Tb_{2+x}Ti_{2-x}O_{7-y}$ crystals, taking into account the fields of random deformations induced by point defects of the crystal lattice. Modeling of the spectra within the single-ion approximation allowed us to satisfactorily reproduce the available experimental studies of absorption profiles for radiation with the wave vector $\mathbf{q} \parallel [111]$ and magnetic field $\mathbf{h} \parallel [11-2]$ in the crystal with a non-stoichiometric composition ($x = -0.0025$) and a fragment of the neutron scattering spectrum in the range of low transfer energies (1 cm^{-1}) in a crystal with the parameter $x \simeq 0$. The spectral lines considered correspond to quantum transitions between the sublevels of the two lower non-Kramers doublets of Tb^{3+} ions in the crystal field of D_{3d} symmetry, split by random deformations, in the absorption spectra and between the sublevels of the ground doublet in the neutron scattering spectrum. The width of the deformation distribution function ($6.5 \cdot 10^{-4}$ and $2.6 \cdot 10^{-5}$ in crystals of different composition), determined from a comparison of the calculated and measured spectra, agrees with the previously obtained estimates of the width of the deformation distribution functions in dielectric crystals activated by rare-earth ions [22, 25].

In order to reproduce the dependence of the relative intensities of the four components of the broad absorption line on the polarization of terahertz radiation, it is necessary to take into account the possibility of lifting the ban on electric dipole transitions due to displacements of Tb^{3+} ions from the nodes of the regular lattice near defects, accompanied by the appearance of an odd component of the crystal field, and to go beyond the single-particle approximation by including anisotropic exchange [38], magnetic dipole-dipole and electric multipole (in particular, quadrupole [39]) interactions between Tb^{3+} ions in the Hamiltonian of the system under consideration.

Funding. This work was funded by the subsidy allocated to Kazan Federal University for the state assignment in the sphere of scientific activities (Project № FZSM-2024-0010).

REFERENCES

1. M. J. P. Gingras, B. C. den Hertog, M. Faucher, et al., Phys. Rev. B **62**, 6496 (2000).

2. Y.-J. Kao, M. Enjalran, A. Del Maestro, et al., Phys. Rev. B **68**, 172407 (2003).

3. S. R. Dunsiger, R. F. Kiefl, J. A. Chakhalian, et al., Physica B **326**, 475 (2003).

4. S. A. Klimin, J. Magn. Magn. Mater. **383**, 237 (2015).

5. M. Ruminy, E. Pomjakushina, K. Iida, et al., Phys. Rev. B **94**, 024430 (2016).

6. I. V. Alexandrov, L. G. Mamsurova, K. K. Pukhov, et al., JETP Lett. **34**, 68 (1981).

7. T. Fennell, M. Kenzelmann, B. Roessli, et al., Phys. Rev. Lett. **112**, 017203 (2014).

8. A. A. Turrini, M.Ruminy, F. Bourdarot, et al., Phys. Rev. B **104**, 224403 (2021).

9. B. C. den Hertog and M. J. P. Gingras, Phys. Rev. Lett. **84**, 3430 (2000).

10. S. Petit, P. Bonville, J. Robert, et al., Phys. Rev. B **86**, 174403 (2012).

11. S. Guitteny, J. Robert, P. Bonville, et al., Phys. Rev. Lett. **111**, 087201 (2013).

12. Y. Alexanian, J. Robert, V. Simonet, et al., Phys. Rev. B **107**, 224404 (2023).

13. K. Amelin, Y. Alexanian, U. Nagel, et al., Phys. Rev. B **102**, 134428 (2020).

14. E. Constable, R. Ballou, J. Robert, et al., Phys. Rev. B **95**, 020415 (2017).

15. Y. Chapuis, A. Yaouanc, P. D. de Réotier, et al., Phys. Rev. B **82**, 144435 (2010).

16. Y. Chapuis, PhD diss, Université Joseph Fourier, Grenoble (2009).

17. T. T. A. Lummen, I. P. Handayani, M. C. Donker, et al., Phys. Rev B. **77**, 214310 (2008).

18. K. A. Ross, Th. Proffen, H. A. Dabkowska, et al., Phys. Rev. B **86**, 174424 (2012).

19. T. Taniguchi, H. Kadowaki, H. Takatsu, et al., Phys. Rev. B **87**, 060408 (2013).

20. J. D. Eshelby, Phys. Solid State **3**, 79 (1956).

21. M. A. Ivanov, V. Y. Mitrofanov, L. D. Falkovskaya, et al., J. Magn. Magn. Mater. **36**, 26 (1983).

22. B. Z. Malkin, D. S. Pytalev, M. N. Popova, et al., Phys. Rev. B **86**, 124406 (2012).

23. B. Malkin and V. Klekovkina, in Book of abstracts, 7th International Conference on the Highly Frustrated Magnetism, Cambridge University, Warwick (2014), p. 91.

24. N. Martin, P. Bonville, E. Lhotel, et al., Phys. Rev. X **7**, 041028 (2017).

25. B. Z. Malkin, N. M. Abishev, E. I. Baibekov, et al., Phys. Rev. B **96**, 014116 (2017).

26. Y. Nii, Y. Hirokane, S. Nakamura, et al., Phys. Rev. B **105**, 094414 (2022).

27. Y. Gritsenko, S. Mombetsu, P. T. Cong, et al., Phys. Rev. B **102**, 060403 (2020).

28. V. V. Klekovkina, N. M. Abishev, Opt. Spectrosc. **131**, 454 (2023).

29. L. K. Aminov, B. Z. Malkin, and M. A. Teplov, *Magnetic properties of nonmetallic lanthanide compounds*. In: Handbook on the Physics and Chemistry of the Rare-Earths, v. 22, 1996, ed. K.A. Gschneidner and LeRoy Eyring, North-Holland, Amsterdam, pp. 295-506.

30. Y. Luan, *Elastic properties of complex transition metal oxides studied by Resonant Ultrasound Spectroscopy*, PhD diss., University of Tennessee, Tennessee (2011). http://trace.tennessee.edu/utk_graddiss/993

31. W. T. Carnall, G. L. Goodman, K. Rajnak, et al., J. Chem. Phys. **90**, 3443 (1989).

32. V. V. Klekovkina, A. R. Zakirov, B. Z. Malkin, et al., J. Phys.: Conf. Ser. **324**, 012036 (2011).

33. B. Z. Malkin, in Spectroscopy of Solids Containing Rare Earth Ions, ed. by A. A. Kaplyanskii, R. M. Macfarlane, NorthHolland, Amsterdam (1987), p. 13.

34. E. Lhotel, C. Paulsen, P. Dalmas de Reotier, et al., Phys. Rev. B **86**, 020410(R) (2012).

35. V. V. Klekovkina, B. Z. Malkin, Opt. Spectrosc. **116**, 925 (2014).

36. E. Kermarrec, D. D. Maharaj, J. Gaudet, et al., Phys. Rev. B **92**, 245114 (2015).

37. H. Takatsu, H. Kadowaki, T. J. Sato, et al., J. Phys.: Condens. Matter **24**, 052201 (2012).

38. B. Z. Malkin, T. T. A.Lummen, P. H. M. van Loosdrecht, et al., J. Phys.: Condens. Matter **22**, 276003 (2010).

39. H. Takatsu, S. Onoda, S. Kittaka, et al., Phys. Rev. Lett. **116**, 217201 (2016).